

Submitted to Journal of Geophysical Research, 27 June, 1999. Resubmitted, 2 May, 2000.

## Ionospheric HF pump wave triggering of local auroral activation

N. F. Blagoveshchenskaya,<sup>1</sup> V. A. Kornienko,<sup>1</sup> T. D. Borisova,<sup>1</sup> B. Thidé,<sup>2</sup>  
M. J. Kosch,<sup>3</sup> M. T. Rietveld,<sup>3</sup> E. V. Mishin,<sup>4</sup> R. Yu. Luk'yanova,<sup>1</sup> and  
O. A. Troshichev<sup>1</sup>

### Abstract.

Experimental results from Tromsø HF pumping experiments in the nightside auroral  $E$  region are reported. We found intriguing evidence that a modification of the ionosphere-magnetosphere coupling, due to the effects of powerful HF waves beamed into an auroral sporadic  $E$  layer, can lead to a local intensification of the auroral activity. Summarizing multi-instrument ground-based observations and observations from the IMP 8 and IMP 9 satellites, one can distinguish the following peculiarities related to this auroral activation: modification of the auroral arc and its break-up above Tromsø; local changes of the horizontal currents in the vicinity of Tromsø; increase of the electron temperature and ion velocities at altitudes above the HF pump reflection level; distinctive features in dynamic HF radio scatter Doppler spectra; pump-induced electron precipitation; substorm activation exactly above Tromsø. The mechanisms of the modification of the ionosphere-magnetosphere coupling through the excitation of the turbulent Alfvén boundary layer between the base of the ionosphere ( $\sim 100$  km) and the level of sharp increase of the Alfvén velocity (at heights up to one Earth radius), and the formation of a local magnetospheric current system are discussed. The results suggest that a possible triggering of local auroral activation requires specific geophysical conditions.

### Introduction

Field-aligned currents (FACs) play an important rôle in the process of energy transfer between the magnetosphere and the ionosphere. They establish the force balance between the hot, tenuous plasma of the magnetosphere and the cold, dense plasma of the ionosphere [Haerendel, 1990]. Important agents in the magnetosphere-ionosphere coupling are Alfvén waves, since they are equivalent to time-varying field-aligned currents. It has been suggested that the static coupling is dominant for large-scale magnetosphere-ionosphere coupling, while the Alfvén wave coupling is dominant for small-scale coupling [Nagatsuma *et al.*, 1996]. One of the most remarkable manifestations of the dynamic processes in the solar wind-magnetosphere-ionosphere system is the substorm phenomenon. It is known that a magnetospheric substorm involves two components: the directly driven component, and the energy storage release part. The driven system responds directly to changes in the interplanetary medium (IMF orientation, solar wind pressure) and in-

volves the direct deposition of solar wind energy into the auroral ionosphere and the symmetric ring currents. The storage-release system pertains to the process of storage of energy in the tail magnetic field and in the kinetic drift of the magnetotail particles. After that, it is explosively released into the auroral ionosphere and symmetric ring current system [Rostoker *et al.*, 1987; Rostoker, 1999]. As pointed out by Rostoker [1999] the progress of the substorm may be produced by either the more global, directly driven process or a more localized, storage-release process and may be looked at either on a global scale or on a local scale.

During a substorm onset, the large-scale laminar magnetospheric convection is disrupted because the magnetospheric cross-tail current is diverted down the magnetic field lines [McPherron *et al.*, 1973]. This leads to the activation of the substorm current loop, the so-called substorm current wedge [Kamide and Baumjohann, 1993; Rostoker *et al.*, 1987]. Boström [1964] proposed two auroral current systems connected to the auroral electrojet. This model has not only remained valid up to present time, but also comprises most suggestions made later on.

At the ionospheric level the substorm expansion onset is characterized by brightening and subsequent break-up of a pre-existing auroral arc [Akasofu, 1964]. There are indica-

<sup>1</sup>Arctic and Antarctic Research Institute, St. Petersburg, Russia.

<sup>2</sup>Swedish Institute of Space Physics, Uppsala Division, Sweden.

<sup>3</sup>Max-Planck-Institut für Aeronomie, Katlenburg-Lindau, Germany.

<sup>4</sup>MIT Haystack Observatory, Westford, Mass., USA

tions that some auroral arcs are generated by field line resonances (FLRs) [Samson et al., 1996].

Lui and Murphree [1998] proposed a substorm onset model by combining a theory of the auroral arc generation due to FLRs with a theory of current disruption in the near-Earth magnetic tail based on the cross-field current instability. It allows a close tie of current disruption region in the magnetotail to the location of the auroral arc.

In recent times, it has been generally assumed that the ionosphere plays a rather passive rôle in the substorm process. Nonetheless, some exceptions to this assumption exist. Firstly, models emphasizing changes in the ionospheric conductivity proposed by Kan and Sun [1985], Kan [1993], and Lysak [1990], and its rôle in enhancing the field-aligned currents Lysak and Song [1998]. Secondly, models which emphasized the decoupling of magnetospheric convection from the ionosphere, induced by the formation of parallel electric fields [Haerendel, 1990]. Lastly, there are models which emphasize the excitation of the turbulent Alfvén boundary layer in the polar ionosphere, thus giving rise to a strong turbulent heating of the plasma and to the production of accelerated particles [Trakhtengerts and Feldstein, 1991].

To prove the active rôle of the auroral ionosphere in the substorm process, the controlled injection of high-power radio waves into space from purpose-built ground-based HF radio facilities has constituted an excellent tool.

Experimental results concerning artificial modification of the ionosphere-magnetosphere system by HF pump waves were presented by Blagoveshchenskaya et al. [1998, 1999].

In this paper we report experimental results from Tromsø HF pumping experiments in the nightside auroral  $E$  region and present evidence for a modification, produced by powerful HF radio waves, of the ionosphere-magnetosphere coupling, leading to a local intensification of the auroral activity. Data from bistatic HF Doppler radio scatter, the IMAGE magnetometer network, the EISCAT UHF radar, the Tromsø dynasonde, the digital all-sky imager (DASI), and the IMP 8 and IMP 9 satellites were used in the analysis.

## Experimental methods and equipment used

The experiments reported here were conducted by using the EISCAT HF heating facility [Rietveld et al., 1993] located near Tromsø (geographical coordinates  $69.6^\circ\text{N}$ ,  $19.2^\circ\text{E}$ ,  $L = 6.2$ , magnetic dip angle  $I = 78^\circ$ ) in the pre-midnight hours of February 16 and 17, 1996. The Tromsø heater was operating at the frequency 4040 kHz,  $O$ -mode polarization, and an effective radiated power of 150 MW. The antenna beam was tilted  $6^\circ$  to the south, thus allowing HF pumping in a near field-aligned direction.

Bistatic scatter measurements of HF diagnostic signals were carried out on the London–Tromsø–St. Petersburg path at operational frequencies of 9410 and 12,095 kHz. The analysis of the received diagnostic waves, scattered from artificial field-aligned irregularities (AFAIs) above Tromsø, was made with a Doppler spectral method in St. Petersburg

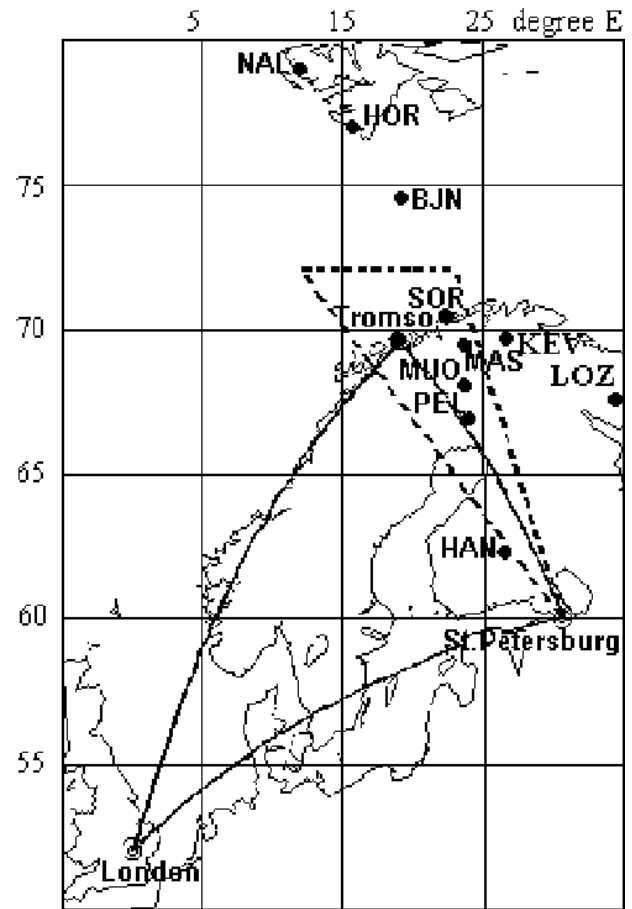


**Figure 1.** General view of the experiment geometry, indicating the position of the London–Tromsø–St. Petersburg path, where HF Doppler measurements of the HF signals scattered from AFAIs were made, and the locations of the IMAGE magnetometer stations. The names of the stations used are as follows: Ny Ålesund (NAL;  $78.92^\circ\text{N}$ ,  $11.95^\circ\text{E}$ ), Hornsund (HOR;  $77.00^\circ\text{N}$ ,  $15.60^\circ\text{E}$ ), Bear Island (BJN;  $74.50^\circ\text{N}$ ,  $19.20^\circ\text{E}$ ), Sørøya (SOR;  $70.54^\circ\text{N}$ ,  $22.22^\circ\text{E}$ ), Tromsø (TRO;  $69.66^\circ\text{N}$ ,  $18.94^\circ\text{E}$ ), Masi (MAS;  $69.46^\circ\text{N}$ ,  $23.70^\circ\text{E}$ ), Muonio (MUO;  $68.02^\circ\text{N}$ ,  $23.53^\circ\text{E}$ ), Pello (PEL;  $66.90^\circ\text{N}$ ,  $24.08^\circ\text{E}$ ), Hankasalmi (HAN;  $62.30^\circ\text{N}$ ,  $26.65^\circ\text{E}$ ), Kevo (KEV;  $69.76^\circ\text{N}$ ,  $17.01^\circ\text{E}$ ), and Lovozero (LOZ;  $67.97^\circ\text{N}$ ,  $22.22^\circ\text{E}$ ).

at a distance of about 1200 km; the receiving antenna was directed toward Tromsø. The geometry of the experiments is shown in Figure 1. Spectral processing of the diagnostic signals was made with a Fast Fourier Transform (FFT) method. On the 16 and 17 February, the frequency bandwidth used was 50 and 33 Hz, respectively, with a frequency resolution of about 0.1 Hz and a temporal resolution of about 10 s.

To facilitate the interpretation of the Doppler measurements, we used data from the IMAGE magnetometer network [Lühr et al., 1996]. The locations of the IMAGE magnetometers are depicted in Figure 1. The time resolution of the IMAGE magnetometers used in this study was 10 s.

The information about disturbances in the interplanetary magnetic field (IMF) and in the solar wind, that could be related with the substorm onset, was obtained from IMP 8 and IMP 9 satellite data. The time resolution of the satellite data used in this study was 1 minute.

Optical data were obtained with the digital all-sky imager (DASI). Details of the instrumentation can be found in the work by *Kosch et al.* [1998]. The DASI is located at Skibotn, near Tromsø (69.3°N, 20.4°E). In this study we used 557.7 nm data with 10 s and 30 s temporal resolution.

To obtain information about changes of the electron densities and temperatures,  $N_e$  and  $T_e$ , and ion temperatures and velocities,  $T_i$  and  $V_i$ , during HF pumping experiments, EISCAT UHF radar measurements at Tromsø were also employed.

## Observational results

The Tromsø dynasonde ionograms as well as the altitude-temporal variations of the electron density measured by the EISCAT UHF radar in course of the Tromsø pumping experiments on February 16 and 17, 1996, show the presence of an intense sporadic  $E_s$  layer with a maximum plasma frequency of  $4.1 \leq f_0E_s \leq 4.5$  MHz at heights  $100 \leq h_mE_s \leq 110$  km. We therefore conclude that the  $E$  region of the auroral ionosphere was actually the region where the powerful HF radio waves were reflected. This led to the generation of artificial field-aligned irregularities (AFAIs) which scattered the 9 and 12 MHz signals used for Doppler diagnostics. It is believed [*Djuth et al.*, 1985; *Noble et al.*, 1987] that a thermal resonance instability at the upper-hybrid (UH) level is the strongest candidate for the excitation of AFAIs in the  $E$  region. It should be noted that, under the specific conditions when the pump waves are reflected from auroral  $E_s$  layers, the pump reflection height is close to the altitude of the heater-enhanced conductivity region which coincides with the auroral electrojet; see the review article by *Stubbe* [1996] and references therein. This means that the plasma resonance level was close to the altitude of the heater-enhanced conductivity region.

### Experiment on February 17, 1996

The experiment on February 17, 1996, was conducted from 20 to 23 UT with a 4 min on, 6 min off HF cycle. A very interesting observation in this experiment is the behavior of the auroral arc in the vicinity of Tromsø during the heating cycle 20:30–20:34 UT; see the DASI data in Plate 1. Beginning at 20:32 UT (third row in Plate 1), a gradual thinning of the auroral arc, accompanied by the appearance of a weak bulge above Tromsø, is observed. Thereafter the brightening and subsequent breakup of the arc 20:33.40 UT takes place exactly above Tromsø.

The magnetic field  $X$ ,  $Y$ , and  $Z$  components, as recorded by the NAL, HOR, BJN, SOR, TRO, MAS, MUO, PEL, and HAN stations of the IMAGE magnetometer network, are displayed in Figure 2; *cf.* also Figure 1. It can be seen that a

substorm activation started at 20:00 UT. A second activation started at 20:33 UT, indicated by a large negative spike in the magnetic  $X$  component, localized in a narrow latitudinal region around Tromsø, from the SOR to the MAS station.

Examination of the peculiarities in the behavior of the  $X$  and  $Z$  magnetic components in Figure 2 shows that a new westward electrojet appeared at 20:33 UT exactly above Tromsø (reversal of the  $Z$  component from positive values at SOR to negative values at MAS, with  $Z \approx 0$  at the TRO station), and maximal negative amplitude of the  $X$  component ( $X_{\max} = -130$  nT at Tromsø). Thereafter, at 20:38 UT, a large substorm started at higher latitudes ( $X_{\max} = -400$  nT at the HOR station). We will only consider the substorm activation around Tromsø which started at 20:33 UT.

Studies of magnetograms from the Kevo (Figure 3) and Lovozero (Figure 4) stations, which are both located further east of Tromsø, clearly show that an intensity of the magnetic disturbance is decreasing with distance from Tromsø. Hence, we can safely conclude that the substorm really occurred above Tromsø.

The behavior of the equivalent current vectors (from the  $X$  and  $Y$  magnetic components in Figure 2), describing the distribution of the magnetic disturbances from 20:29 to 20:36 UT, is summarized in Figure 5. It is clearly seen that the most drastic changes of the current directions and magnitudes in the vicinity of Tromsø from SOR to MAS occurred during the period 20:33–20:34 UT.

It is well established that the onset of a substorm can be related to disturbances in the interplanetary magnetic field (IMF) and/or in the solar wind. Because of that it is of interest to consider the IMF and solar wind data during heating experiment. The behavior of  $B_x$ ,  $B_y$ , and  $B_z$  components of the IMF as well as the solar wind velocity  $V$  from IMP 8 and IMP 9 satellite data is shown in Figure 6.

As is clearly seen from Figure 6, there are no significant changes in the  $B_z$  and  $B_y$  components; during the period 16–22 UT they undergo maximal amplitude fluctuations not exceeding 1.5 nT. Nonetheless, it should be pointed out that small directional changes in the  $B_z$  component (northward turning) accompanied by a  $B_x$  turn from positive to negative values occurred at about 20:35 UT. Therefore, IMF data show an absence of major directional changes in the  $B_z$  and  $B_y$  components which could be associated with the substorm activation at 20:33:40 UT. In this respect, we note the results of detailed observations performed by *Henderson et al.* [1996] and which clearly show that the magnetospheric substorm can indeed occur in the absence of an identifiable driver in either the IMF or the solar wind dynamic pressure. It is suggested that the internal instability in the magnetospheric system could be the possible driver for these substorms.

Figure 7 presents dynamic Doppler spectra of HF diagnostic signals recorded in St. Petersburg in the course of two heating cycles from 20:18 to 20:38 UT. The turning on of the Tromsø heater at 20:20 UT led to the appearance of an addi-

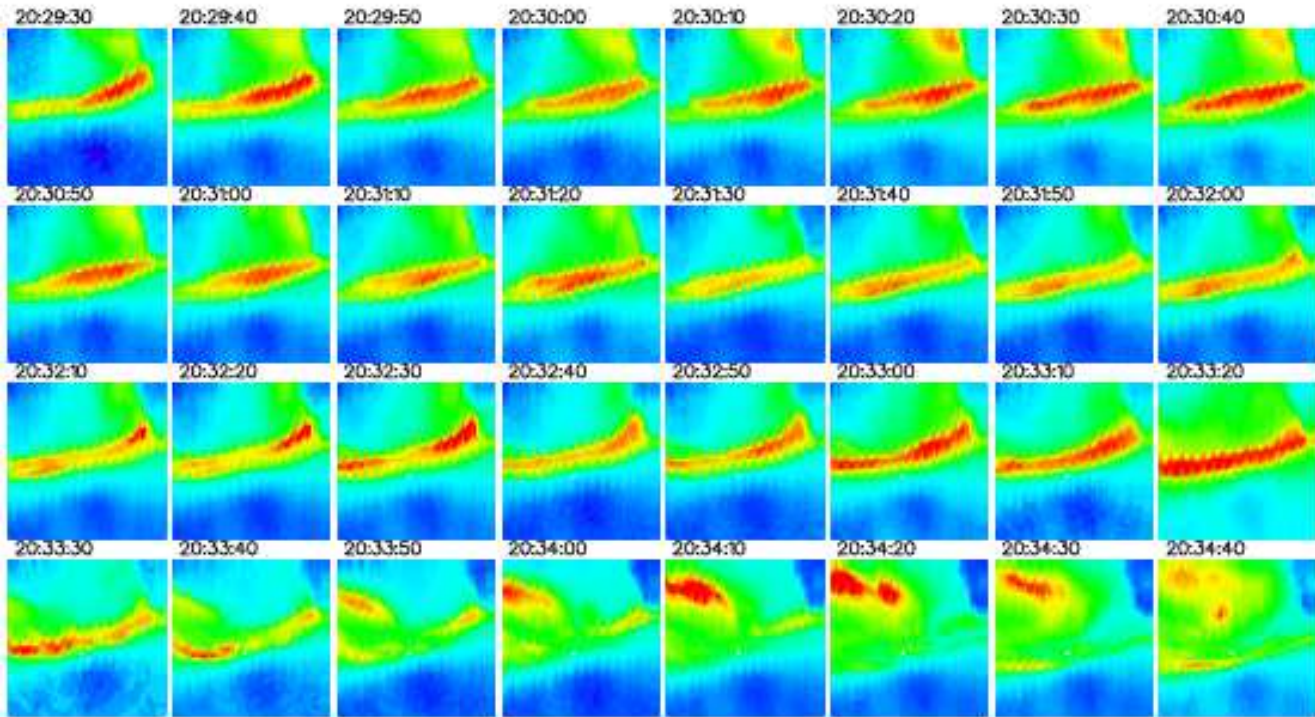


**Plate 1.** A sequence of all-sky imager plots at 557.7 nm obtained near Tromsø on February 17, 1996, from 20:29.30 to 20:34.40 UT. The spatial scale of each plot is  $520 \times 520 \text{ km}^2$ . The white point near the middle of each plot indicates the location of Tromsø. The plot time is 10 s. The Tromsø heater was turned on from 20:30 to 20:34 UT.

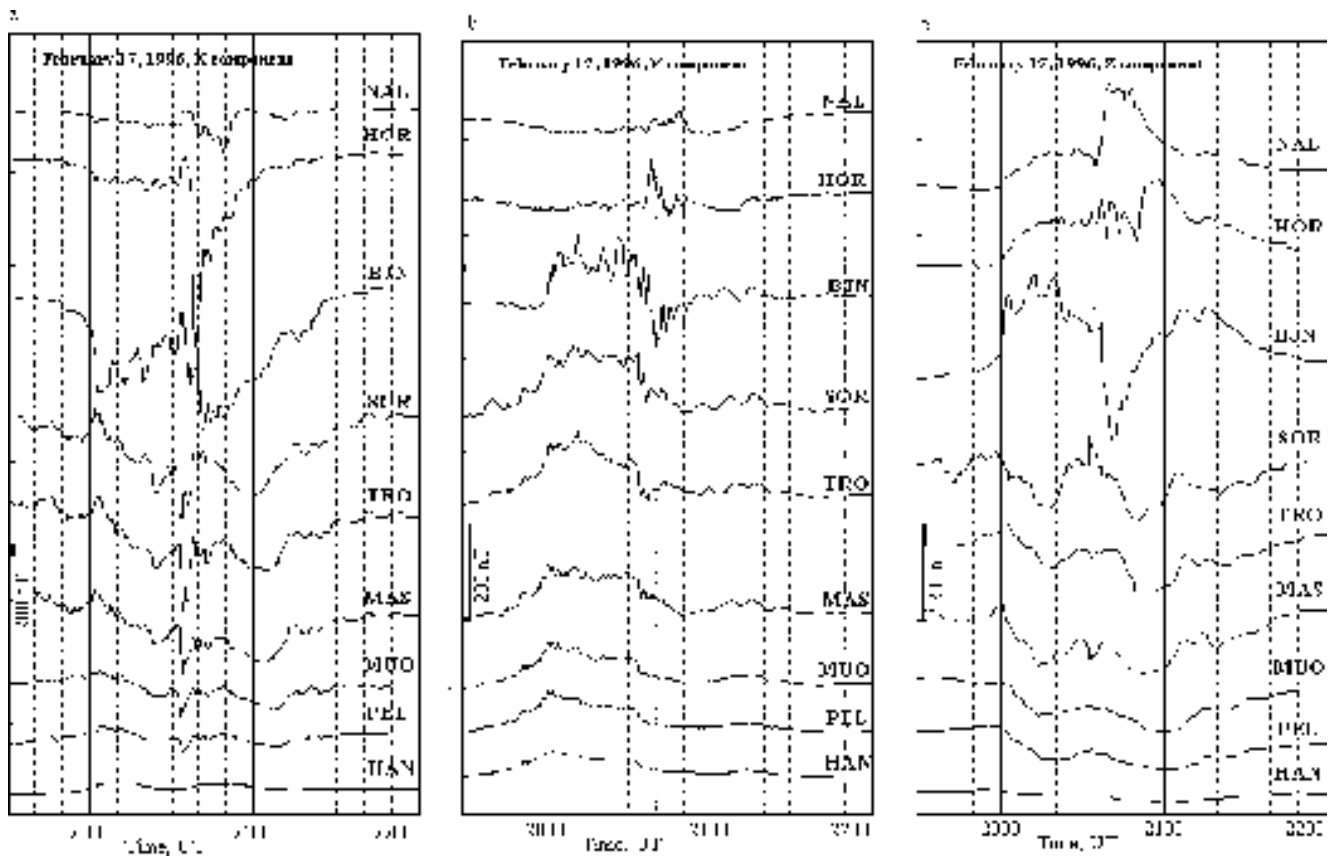


**Figure 2.** The temporal behavior of the X, Y, and Z components of the magnetic field variations on February 17, 1996. Data from the IMAGE magnetometers.

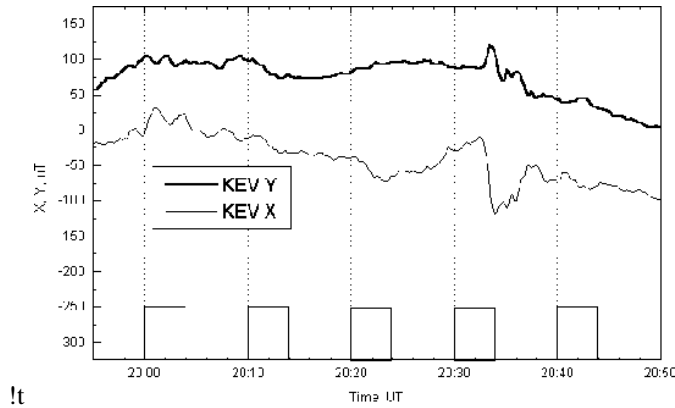


**Figure 3.** Magnetic  $H$  and  $D$  components measured at the Kevo (KEV) magnetic station on February 17, 1996, from 19:55 to 20:50 UT. The heater-on periods are indicated on the bottom axis.

tional track, shifted from the direct signal by about  $-2.5$  Hz. This additional track disappeared after the heater was turned off at 20:24 UT and was produced by diagnostic waves scattered from the artificial field-aligned irregularities (AFAs) generated by the Tromsø HF heating facility in the auroral  $E$  region.

As can also be seen from Figure 7, the heater turn-on at 20:30 UT led to the appearance of field-aligned scattered HF signals in the same manner as in the preceding heating cycle. About 60 s later, wide-band spectral feature occurred throughout the spectral bandwidth analyzed. Thereafter, at 20:33 UT, an additional very intense, short-lived track of about 1 min duration, displaced  $-0.8$  Hz from the main scattered signal, appeared in the Doppler sonogram. The heater turn-off at 20:34 UT was followed by the disappearance of the additional short-lived track, but the AFAI scattered signals, as well as the wide-band spectral features, were maintained for yet another minute.

What is the nature of the wide-band spectral feature closely linked to the auroral activation? It is known that one of the most common features in HF pumping experiments is the generation of Stimulated Electromagnetic Emissions (SEE) [Thidé *et al.*, 1982, 1983, 1989; Thidé, 1990; Stubbe *et al.*, 1984; Leyser *et al.*, 1994]. Unfortunately, no SEE diagnostics capability was available during the experiments so it was not possible to establish directly whether the basic SEE component was excited or not.

The long-delayed effect of about one minute duration, of the wide-band feature observed after the heater turn-off is not clear. Because of this we do not exclude the possibility that this heater-related emission in our experiment is a heater-modified natural auroral emission in the decameter range [LaBelle *et al.*, 1995; Weatherwax *et al.*, 1995].

Another possible explanation is that the observed heater-related wide-band features are accompanied by the excitation of VLF waves and turbulence, known to be excited in ionospheric HF pumping. As was concluded by Vas'kov

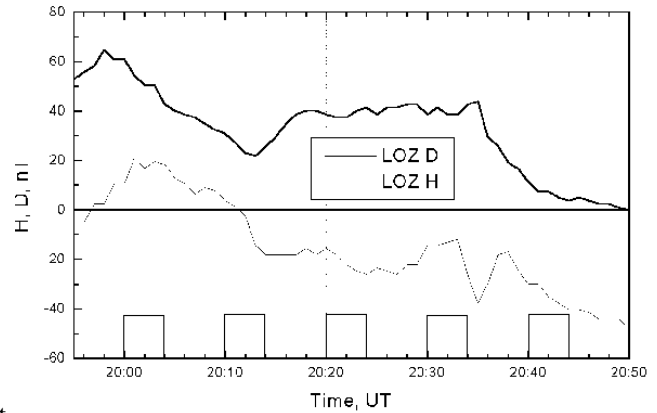


**Figure 4.** Magnetic  $X$ ,  $Y$ ,  $Z$  components measured at the Lovzero (LOZ) magnetic station on February 17, 1996, from 19:55 to 22:50 UT. The heater-on periods are indicated on the bottom axis.

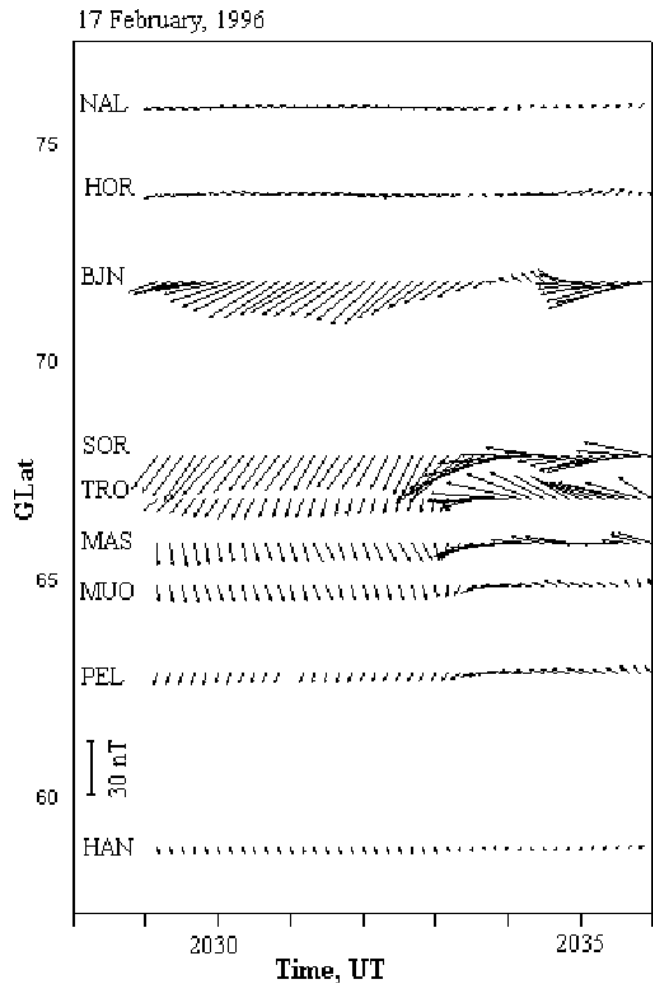


**Figure 5.** The behavior of the equivalent current vectors on February 17, 1996, from 20:29 to 20:36 UT, describing the distribution of magnetic disturbances at the IMAGE network. The heater-on period was from 20:30 to 20:34 UT.

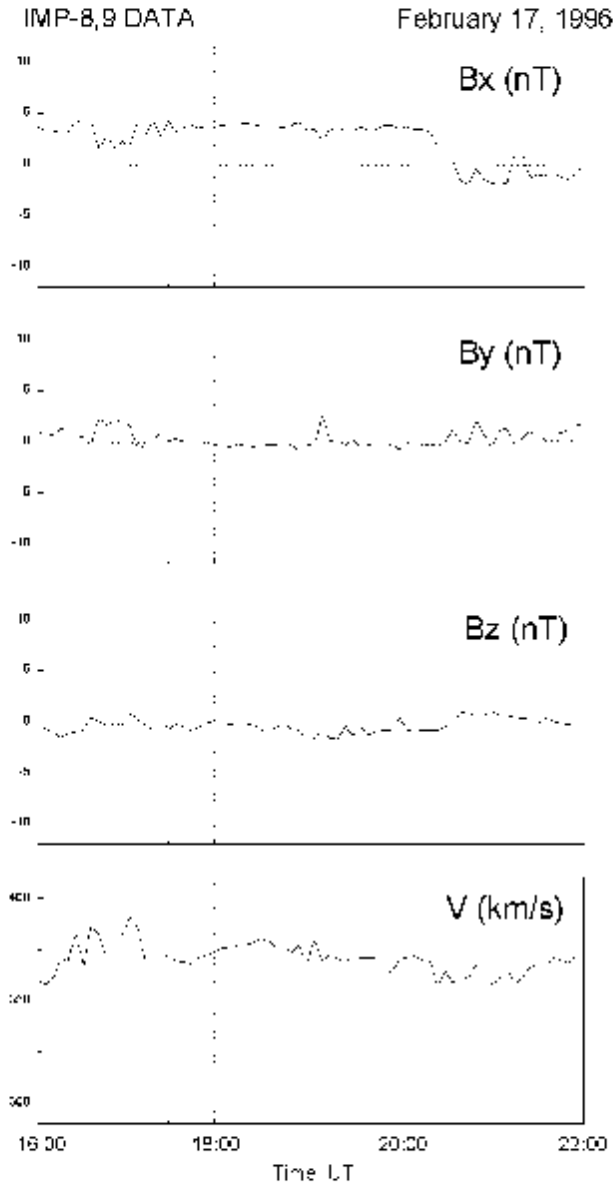


**Figure 6.** The behavior of the  $B_x$ ,  $B_y$ , and  $B_z$  components of the interplanetary magnetic field, and the velocity of the solar wind, on February 17, 1996, from 16 to 22 UT. IMP 8 and IMP 9 satellite data.

et al. [1998] from satellite experiments during the action of un-modulated powerful HF radio waves on the nightside ionospheric  $F$  region, VLF waves may be excited due to a decay process taking place near the pump wave reflection region, or due to the interaction with suprathermal electrons, accelerated by the pump-enhanced plasma turbulence. The heater induced VLF waves can be studied by ground-based techniques. On the other hand, HF-excited VLF waves in the whistler mode were detected by satellites in the upper ionosphere and magnetosphere within the magnetic flux tube footprinted on the heating facility [Vas'kov et al., 1998].

Closely related to the wide-band spectral features in the

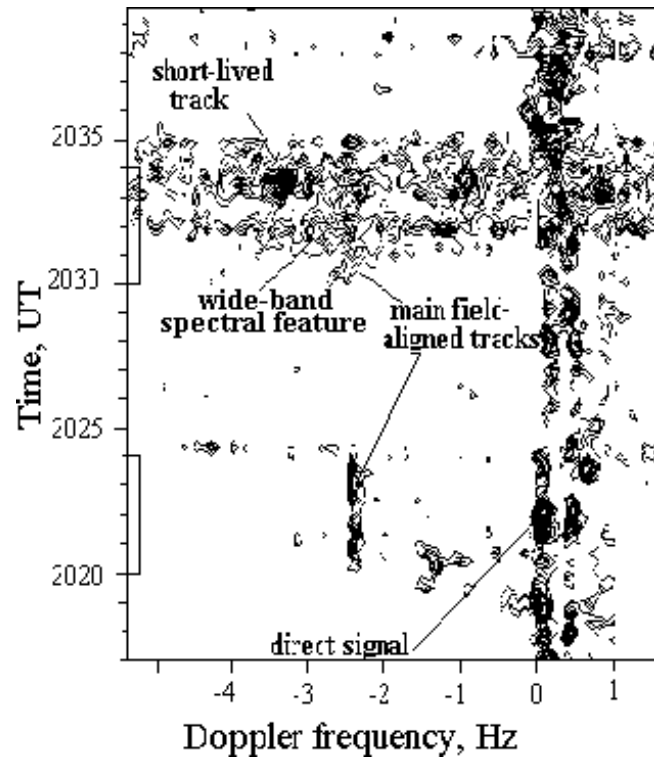


**Figure 7.** Dynamic Doppler spectra of HF diagnostic signals on the London–Tromsø–St. Petersburg path at the operational frequency 12,095 kHz on February 17, 1996, from 20:18 to 20:38 UT. The direct signals propagating from the transmitter to the receiver along a great circle path correspond to zero Doppler shifts. The intervals when the Tromsø heater was turned on are marked on the time axis.

probe wave sidebands was the appearance of an additional short-lived track in the Doppler sonogram. It is likely that this short-lived track was induced by a stimulated precipitation of electrons due to a cyclotron resonant interaction of natural precipitating electrons with heater-induced whistler waves in the magnetosphere [Trefall et al., 1975; Bösinger et al., 1996; Trakhtengerts, 1999]. From the results obtained, we may then conclude that the substorm activation on February 17, 1996, at 20:33 UT exactly above Tromsø was initiated by the pump-induced electron precipitation.

Another interesting peculiarity was detected in the EISCAT UHF radar data (Figure 8). The formation of the electron density cavity took place at 20:33 UT downward from the altitude of about 100 km. It was accompanied by the occurrence of a burst-like increase of the electron density and temperature,  $N_e$  and  $T_e$ , in a wide range of altitudes upward from 110 km. It is well known that an HF pump wave may excite plasma waves and turbulence in the resonant region where the ordinary mode ( $O$ -mode) of the pump wave is reflected from the ionosphere and in the upper hybrid, UH, resonance region. The threshold field strength for the generation, due to ponderomotive force effects, of plasma waves by a powerful  $O$ -mode radio wave is of the

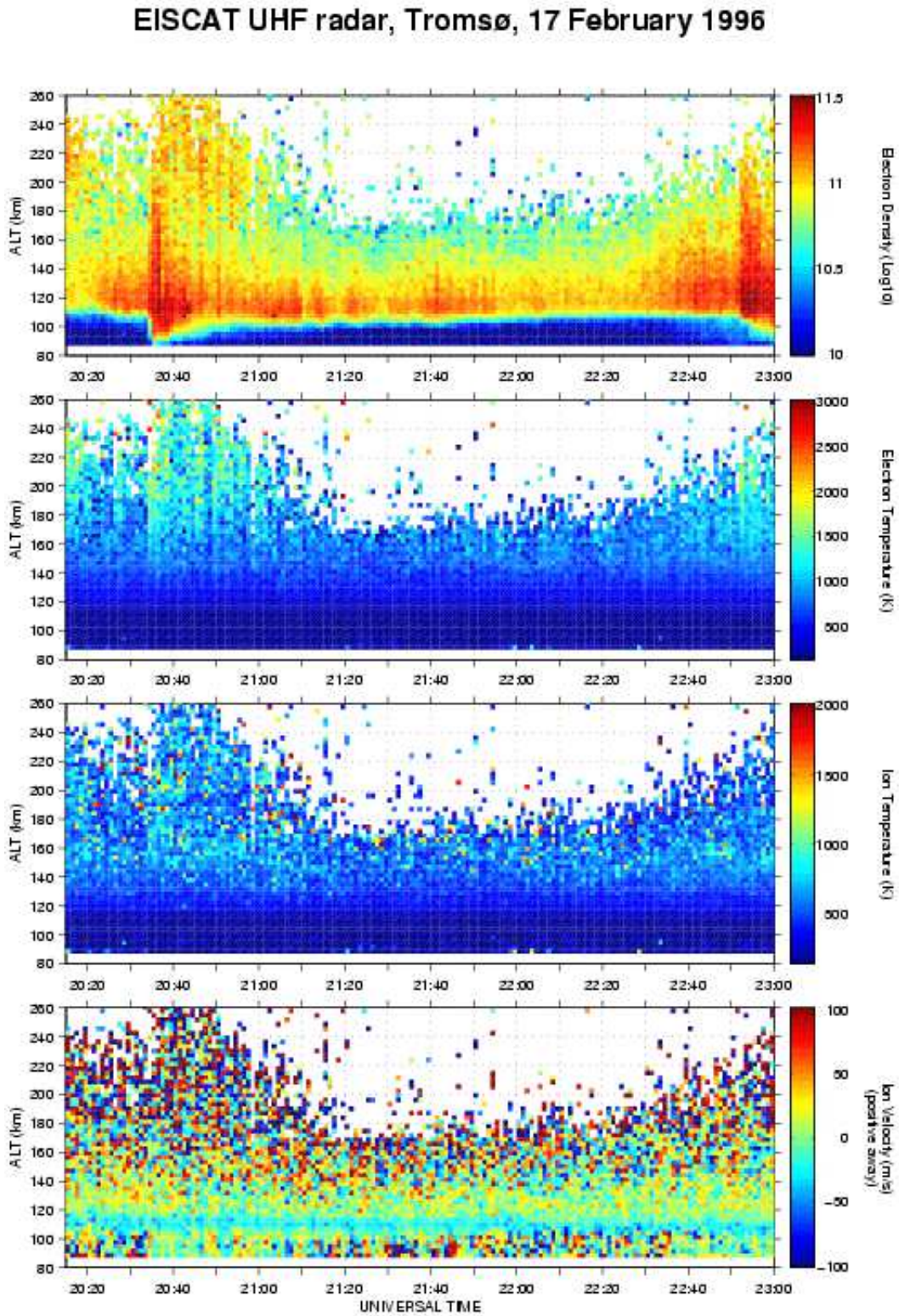


**Figure 8.** Behavior of the electron density, electron and ion temperatures, and ion velocity as observed with the Tromsø EISCAT UHF incoherent scatter radar February 17, 1996, from 20:15 to 23:00 UT, by using a high spatial resolution alternating code (AC). The Tromsø HF heating facility was operated from 20:20 to 23 UT with a 4 min on, 6 min off pump cycle.

order  $E_{\text{th}} \approx 200$  mV/m [Fejer, 1979; Thidé, 1990], a value which was significantly exceeded in our experiments. As was pointed out by Fejer [1979], partial pressure effects can lower this threshold. In these processes, the electrons are assumed to be accelerated and this leads to an electron flux transport along the magnetic field lines [Bernhardt et al., 1988]. Note that the observed changes in the  $N_e$  and  $T_e$  are closely correlated with the auroral activation and may therefore be a signature of the heater-induced precipitation of electrons.

Summarizing the experimental findings from the different ground-based measurements during the heater-on period 20:30–20:34 UT on February 17, one can distinguish the following peculiarities related to the auroral activation observed after 30 minutes from the start of the pumping experiment in the absence of the apparent drivers in the IMF/solar wind parameters: (a) modification of the auroral arc and its break-up above Tromsø; (b) local changes of the horizontal currents in the  $E$  region; (c) generation of scattered Doppler components throughout the whole spectral bandwidth of 33 Hz analyzed; (d) appearance of an additional short-lived Doppler sonogram track, distinct from the main track, corresponding to scattered diagnostic signals due to pump-induced electron precipitation; (e) formation of the cavity in  $N_e$  downward from 100 km and burst-like increase of  $N_e$  and  $T_e$  at heights upward from 110 km; (f) substorm activation exactly above Tromsø.

### Experiment on February 16, 1996

In this section we present data from the Tromsø HF pumping experiment carried out on February 16, 1996, starting at 21:00 UT. The pump wave was modulated with a 4 min on, 6 min off cycle from 21 to 23 UT. This was preceded by some short on periods as the HF transmitter was tuned, from 20:41 to 20:44 UT, from 20:46:30 to 20:48:30 UT, and from 20:52:00 to 20:52:20 UT. The DASI digital all-sky imager data for this day (Plate 2) show that the latitude-oriented auroral arc was located slightly to the south of the heater. It should be pointed out that a most remarkable optical phenomenon was observed during the two heating cycles 21:20–21:24 UT and 21:30–21:34 UT. As can be seen in Plate 2, a development of local spiral-like forms in the auroral arc near Tromsø occurred after the heater was turned on. In the first case (21:20–21:24 UT), the spiral form appeared at 21:21:50 UT and led to the start of an auroral activation. In course of the heater-on period the intensity of this spiral increased and started to decay only after the heater was turned off. In the second case (21:30–21:34 UT), a similar form, but more intense in comparison with the heater-on period 21:20–21:24 UT, appeared at 21:31:20 UT. Furthermore, the brightening and subsequent break-up of an auroral arc at 21:33:50 UT (Plate 2, fourth row, last panel) took place exactly above Tromsø. Such a spiral form can be attributed to the local appearance of field-aligned currents during the heater-on periods 21:20–21:24 UT and 21:30–21:34 UT.

IMAGE magnetograms for the event on February 16,

1996 ( $X$ ,  $Y$ , and  $Z$  magnetic components) are displayed in Figure 9. These magnetic data indicate that the Tromsø heater operation started under quiet magnetic conditions (from 21:00 UT) and that the start of the auroral activation occurred at 21:21 UT during the third heating cycle (21:20–21:24 UT). It should be noted that this event, just as the substorm activation on February 17, 1996, occurred in a narrow latitudinal region localized around Tromsø. This is evident from the behavior of the equivalent current vectors obtained from the IMAGE magnetometers from 21:19 to 21:27 UT (Figure 10). Moreover, the most drastic changes of the current directions and magnitudes were also observed in the vicinity of Tromsø, ranging in latitude from the SOR to the MAS magnetic stations.

The  $B_x$ ,  $B_y$ , and  $B_z$  components of the IMF and the solar wind velocity obtained from IMP 8 and IMP 9 satellite data for the event on February 16, 1996 are shown in Figure 11. Contrary to the event on February 17, a southward turning of the  $B_z$  component of the IMF took place at 20:40 UT. The amplitude of the southward  $B_z$  component was about  $-2$  nT. This small directional change in the  $B_z$  component could possibly be a driver for the auroral activation.

Figure 12 displays the dynamic Doppler spectra obtained on February 16, 1996, from 20:58 to 21:40 UT, on the London–Tromsø–St. Petersburg path, for a radio scatter operational frequency of  $f = 9410$  kHz. One can see that the heater turn-on at 21:10 UT led to the appearance of a weak scattered signal shifted from the direct signal (corresponding to zero Doppler shift) by about  $+6.3$  Hz. Note that the Doppler frequency  $f_d$  of the scattered signal changed during this heater-on period with a maximum magnitude of 2.2 Hz. When the heater was turned off at 21:14 UT, the scattered signals did not disappear as was the case on February 17, 1996. Up to 21:34 UT, intense scattered signals from natural  $E_s$  irregularities were observed in St. Petersburg.

The spectral structure of the signals scattered from AFAIs is quite complicated. It includes a broadening of the Doppler spectra and burst-like noise enhancements. The variations of  $f_d$  with time of the broad part in the dynamic Doppler spectra can be correlated with the movements of the auroral arcs in the vicinity of Tromsø on the line of sight of the radio scatter observations from St. Petersburg.

The noise enhancement occurred over a frequency range of up to 35 Hz, which is below the ion cyclotron frequency. We emphasize that the Doppler measurements in this modification experiment were performed in a limited frequency bandwidth of 50 Hz. At frequencies below the ion cyclotron frequency the only known electromagnetic modes of propagation along magnetic field lines is the Alfvén wave. Thus one would expect that Alfvén waves would be excited by the HF pumping of the night-side auroral  $E$  region. Alfvén waves associated with ELF noise are identified with electric to magnetic field ratios of the order of the Alfvén velocity. These waves are observed to occur in narrow regions typically of the order 1–3 km and have highly irregular wave forms [Gurnett et al., 1984].

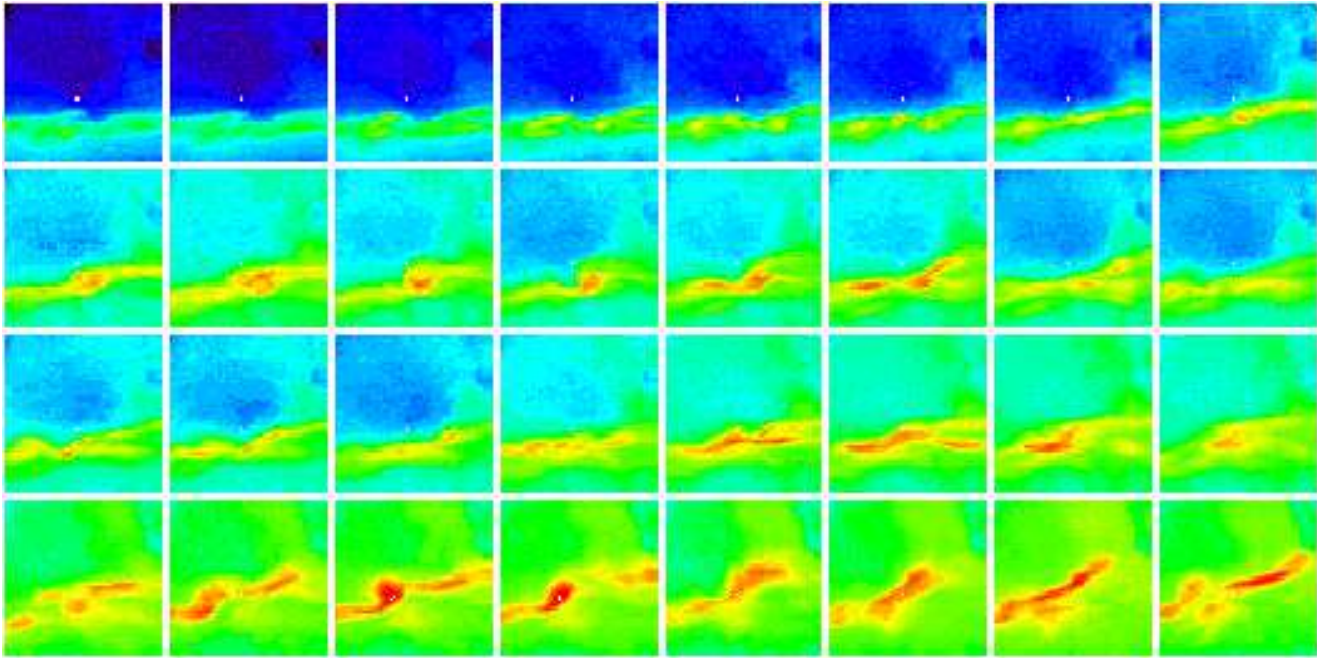


**Plate 2.** A sequence of all-sky imager plots at 557.7 nm obtained near Tromsø on February 16, 1996, from 21:18:20 to 21:33:50 UT. The spatial scale of each plot is the same as in Figure 1. The plot time is 30 s. The Tromsø heater was turned on from 21:20 to 21:24 UT and 21:30 to 21:34 UT.

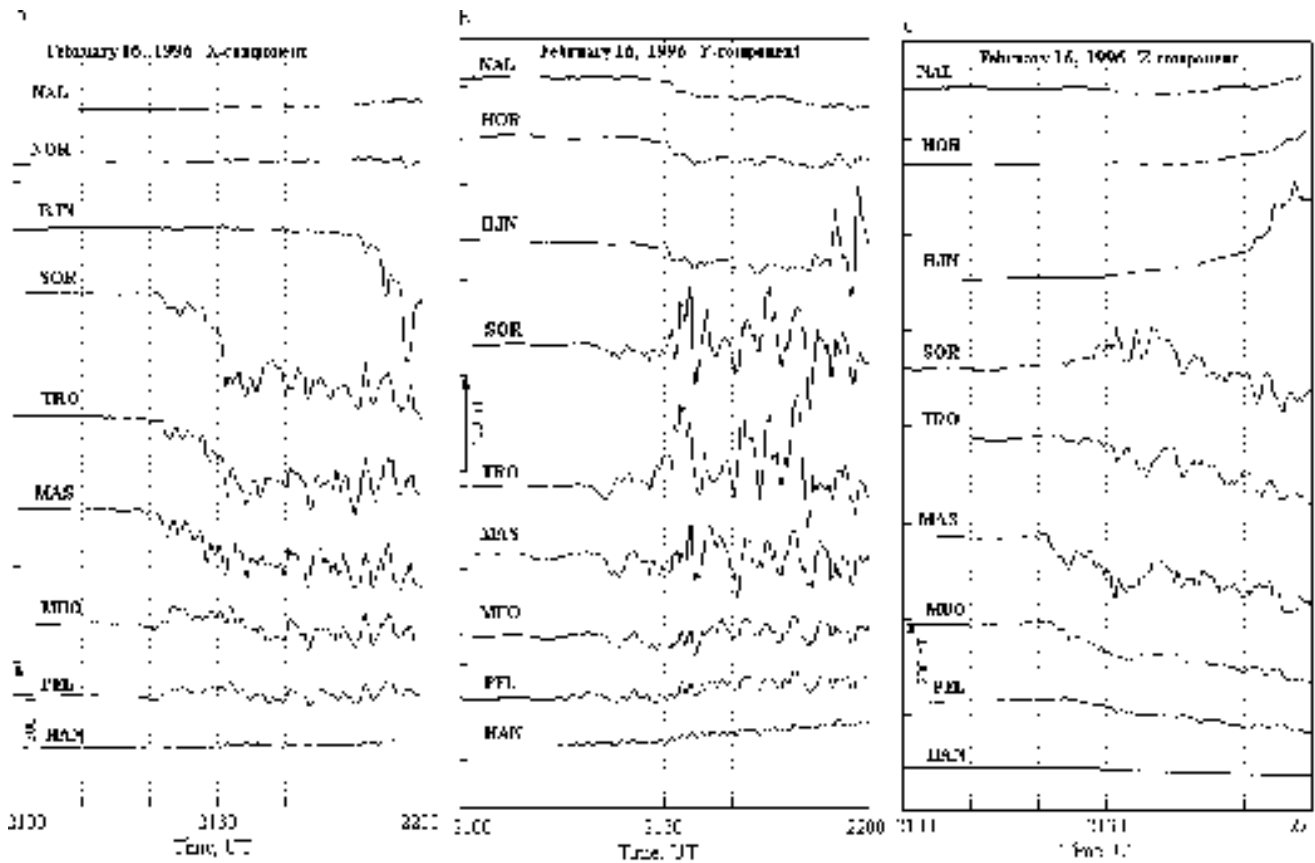


**Figure 9.** The temporal behavior of the X, Y, and Z components of the magnetic field variations on February 16, 1996. Data from the IMAGE magnetometers.

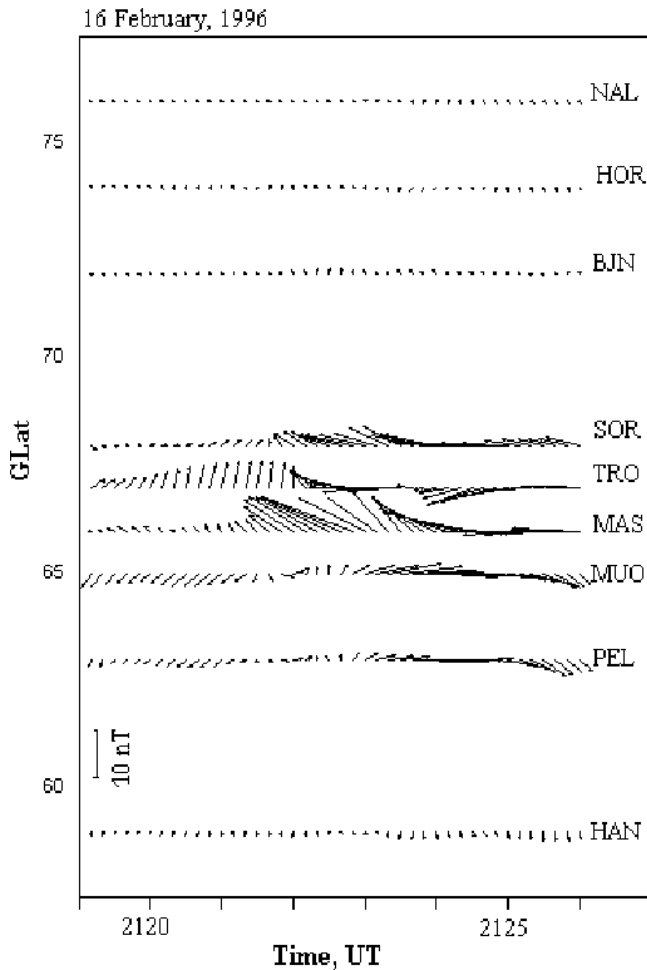


**Figure 10.** The behavior of the equivalent current vectors on February 16, 1996, from 21:19 to 21:27 UT, describing the distribution of magnetic disturbances at the IMAGE network. The heater-on period was from 21:20 to 21:24 UT.

Figure 13 presents EISCAT Tromsø UHF radar data ( $N_e$ ,  $T_e$ ,  $T_i$ , and  $V_i$ ) obtained on February 16, 1996, from 19 to 22 UT. It can be seen from Figure 13 that in the first two consecutive heating cycles from 21:00 to 21:04 UT and 21:10 to 21:14 UT, increases of  $N_e$  and  $T_e$  in the altitude range 120–160 km were clearly observed. Recall that the HF pump wave was reflected from heights of about 100–110 km. Note also the “missing data layer” at about 110 km from 21 to 21:15 UT. This is almost certainly due to data which could not be fitted by the standard program because of enhanced electron temperatures due to a Farley-Buneman instability produced by large drifts of horizontal electric fields. The enhanced ion temperature  $T_i$ , over the whole 120–160 km height range is an evidence of this enhanced field. All these features are recognized phenomena. Therefore, the start of the Tromsø HF heater operation at 21 UT was accompanied by the strong Farley-Buneman instability excitation at the HF pump wave reflection level.

Similar to the event of February 17, 1996, we observed in the EISCAT UHF radar data during the auroral activa-

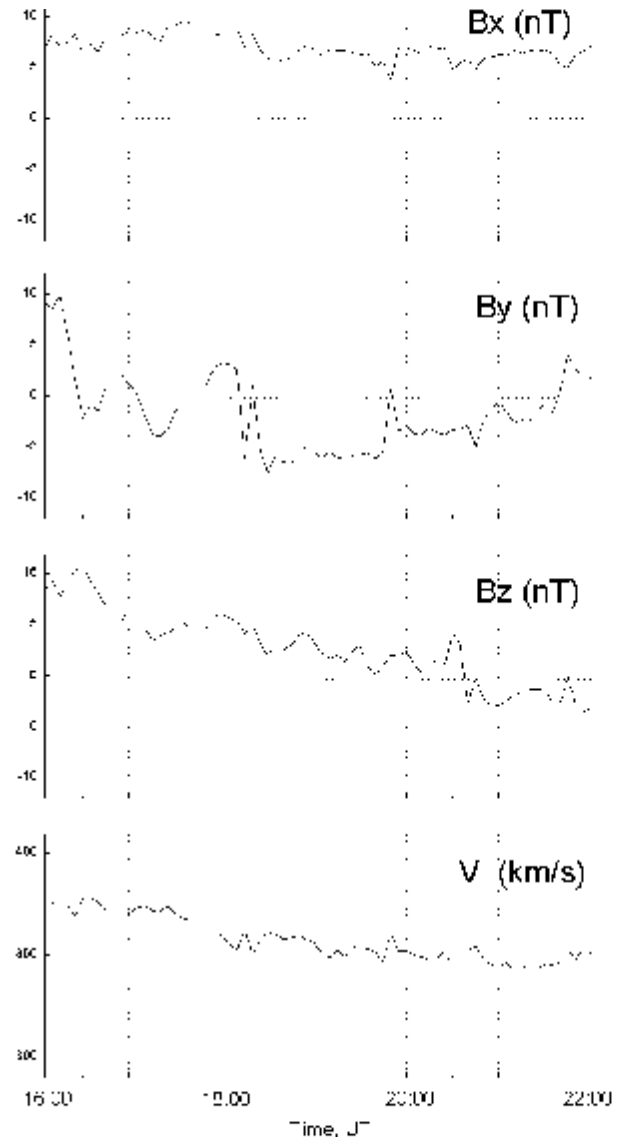


**Figure 11.** The same as in Figure 6 but for February 16, 1996.

tion onset at 21:21 UT a formation of an electron density cavity downward from the height of 110 km. This was accompanied by a burst-like increase of  $N_e$  at altitudes upward from 110 km. Furthermore, once started at about 21:21 UT, the process of the auroral activation development was able maintain itself even when the heater was turned off. This can be seen from Figure 13 which exhibits electron density increases before 21:30 UT, at which time the HF heater was turned off.

From the multi-instrument experimental data from the period 21:20–21:24 UT on February 16, 1996, one can identify the following specific features, which may be related to the auroral activation observed 20 minutes from the start of the HF heater operation in the presence of a small directional

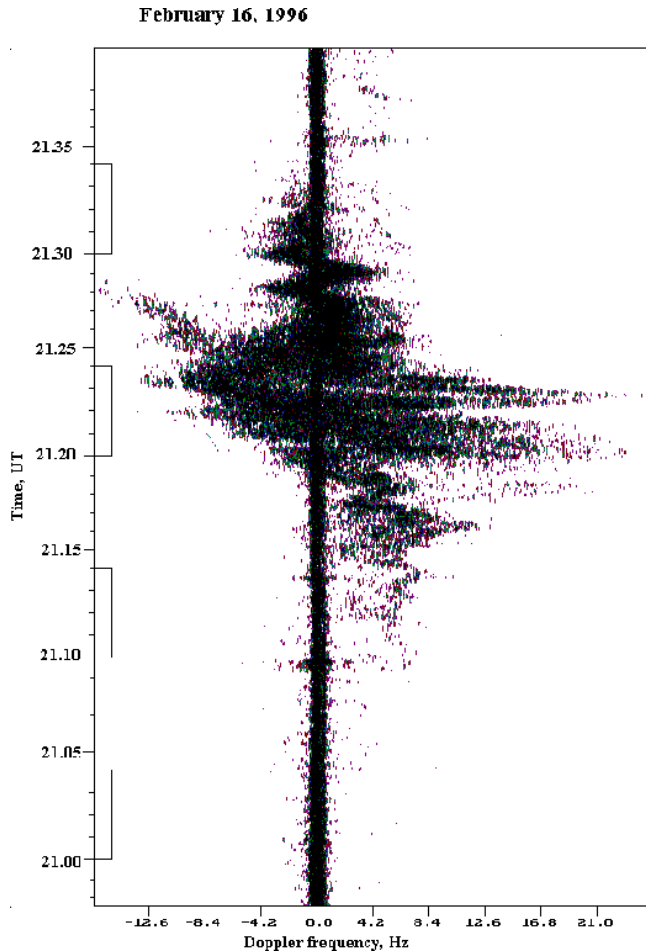


**Figure 12.** Dynamic Doppler spectra of HF diagnostic signals on the London–Tromsø–St. Petersburg path at operational frequency 9410 kHz on February 16, 1996, from 20:58 to 21:40 UT. The intervals when the Tromsø heater was turned on are marked on the time axis.

change of the  $B_z$  component of the IMF: (a) modification of the auroral arc and local spiral-like formation; (b) local changes of the horizontal currents in the  $E$  region in the vicinity of Tromsø; (c) generation of burst-like noise in the frequency range up to 35 Hz; (d) formation of the cavity in  $N_e$  downward from a 110 km level and burst-like increase in  $N_e$  at heights upward from 110 km; (e) substorm activation in the localized latitudinal region above Tromsø.

## Discussion

A bistatic HF Doppler radio scattering setup has been used in conjunction with the IMAGE magnetometer network, the DASI digital all-sky imager, the Tromsø dynasonde, and the EISCAT UHF radar to find evidence that powerful HF radio waves can cause a modification of the ionosphere-magnetosphere coupling which can lead to a local intensification of the auroral activity. Results presented, as obtained from ground-based observations made on two consecutive days, can be interpreted as auroral activations lo-

calized over the Tromsø HF heating facility. In recent times, the possibility of triggering magnetospheric substorms by artificial impacts has been discussed. The artificial localization of a magnetospheric substorm by strong HF radio beams was considered by *Mogilevsky* [1999], based on measurements onboard the INTERBALL-2 (Auroral probe) satellite. From a consideration of results of active experiments, *Foster* [1998] concluded that substorm onsets may be initiated by such actions. A distinctive feature of the experiments reported here is that the HF pump waves were reflected from an auroral  $E_s$  layer. The presence of a sporadic  $E_s$  layer as well as an auroral arc in the vicinity of the Tromsø heating facility are indicative of naturally precipitating electrons with an energy of a few keV.

First of all, it should be mentioned that there are two basic possibilities to locally activate the auroral activity by an artificial ionospheric modification. The simplest one is creating such strong a perturbation that the surrounding currents exceed the threshold for the instability producing energetic electrons. It implies that the height-integrated conductivity,  $\Sigma = \alpha \int N_e(z) dz$ , be changed by a factor of 5–10 inside a region of more than 10 km dimension. This may probably happen during injection of charged particle beams and plasma clouds in the ionosphere (described by *Holmgren et al.* [1980]).

Another possibility initially explored by *Zhulin et al.* [1978] is based on the idea of a positive feedback in the magnetosphere-ionosphere coupling during the substorm growth phase (see different scenarios in [*Kan*, 1993; *Trakhtengerts and Feldstein*, 1991; *Lysak*, 1991]). In this way, an artificially created conductivity perturbation in the  $E$  region grows faster than in the vicinity until a critical value of the field-aligned current (FAC) has been achieved. Note, that in our Tromsø HF pumping experiments, the auroral activations were observed after 20–30 minutes from the start of the HF heater operation. This is a significant indication that a positive feedback mechanism in the magnetosphere-ionosphere coupling is preferred over other mechanisms to produce the local auroral activations by HF pump waves beamed into a sporadic  $E_s$  layer.

During the experiments, local changes of the ionospheric conductivities, and therefore currents in the magnetic flux tube footprinted at Tromsø, were observed. Note that the duration of the HF heater period was 4 min in our HF pumping experiments. In this long-period heating cycle, conductivity changes are produced due to the electron density disturbances. Their effect is much stronger than those of the short-period heating cycles [*Stubbe*, 1996]. The results of calculations for long-period heating cycles have shown that the conductivity perturbations in the HF pump-modified region are the order of  $\delta\Sigma(r) = 2 \text{ S}$  [*Lyatsky et al.*, 1996]. Very drastic local horizontal current changes, closely correlated with auroral activations during the heater-on periods, were seen in the behavior of the equivalent current vectors obtained from the  $X$  and  $Y$  magnetic field components obtained by the IMAGE magnetometer network (see Figures 5 and 10). It is

### EISCAT UHF radar, Tromsø, 16 February 1996

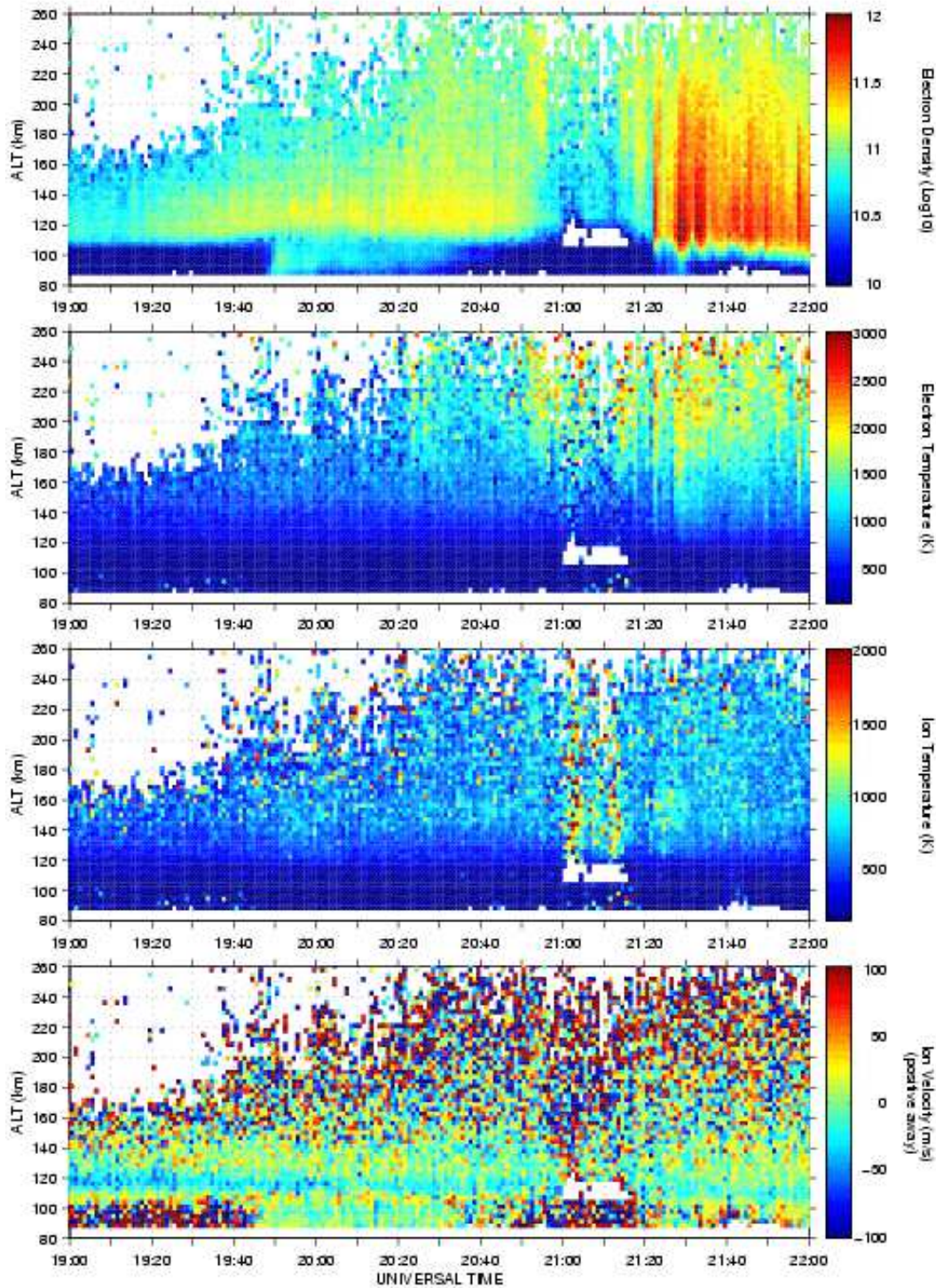


**Figure 13.** Behavior of the electron density, electron and ion temperatures, and ion velocity from Tromsø EISCAT UHF radar measurements on February 16, 1996, from 19 to 22 UT obtained by the use of the high spatial resolution alternating code (AC). The interval from 21 to 21:15 UT with a "missing data layer" at about 110 km is almost certainly data which could not be fitted by the standard program because of enhanced electron temperatures produced by the Farley-Buneman instability due to the large drifts (horizontal electric fields). The enhanced ion temperature over the whole 120–260 km height range is evidence of this enhanced fields. All these features are the recognized phenomena. The Tromsø HF heating facility was operated from 21 to 22 UT with a 4 min on, 6 min off pump cycle.

quite possible that the region of the heater-enhanced ionospheric conductivity was polarized in the background electric field and the polarization electric field propagated into the magnetosphere along the magnetic field lines as the field of an outgoing Alfvén wave [Lyatsky and Maltsev, 1983; Kan and Sun, 1985; Lysak, 1990; Borisov et al., 1996; Kozlovsky and Lyatsky, 1997]. However, other, non-linear processes may also have contributed to the effects observed.

Another phenomenon which accompanied the auroral activations, was the appearance of wide-band spectral features in the Doppler radio scattering data. There are grounds to assume that these spectral features may be associated with pump-induced VLF and ELF noise. Note that these spectral features were observed when the Tromsø heating facility was operated in an 4 min on/6 min off mode, which is a frequency which is significantly lower than that of the waves excited. Therefore, the VLF and ELF noise in our experiments is not the same as the well known effect of ELF and VLF excitation at combination frequencies [Getmantsev et al., 1974; Rietveld et al., 1989]. The emissions observed have other origin. It should be pointed out that VLF and ELF noise propagating into the topside ionosphere over large distances excited by un-modulated HF pump waves were identified for the first time by Vas'kov et al. [1998] in satellite experiments.

It is thought that on February 17, 1996, VLF waves at the harmonics of the lower hybrid frequency were generated by the 150 MW ERP HF waves from the Tromsø heating facility. These VLF waves propagated, in the whistler mode, along the Tromsø magnetic field line into the upper ionosphere. Their interaction with natural precipitation electrons due to a cyclotron resonance, led to a pump-induced precipitation of electrons responsible for the occurrence of additional short-lived track on the Doppler sonogram (see Figure 7). From the results obtained we conclude that a substorm activation exactly above Tromsø at 20:33 UT was initiated by the pump-induced precipitation of the electrons.

One would expect that on February 16, 1996, Alfvén waves were excited by the powerful HF radio waves beamed into night-side auroral E region. These Alfvén waves can be associated with ELF noise enhancement occurring over a frequency range up to 35 Hz (see Figure 12).

It should be noted that the amplification of the interaction between the magnetospheric convection and the ionospheric base is induced by accelerated electrons. What accelerator mechanisms can be caused by HF pumping of the base of the ionosphere at  $\sim 100$  km? It is known [Bernhardt et al., 1988] that electrons are accelerated by the electric potential associated with plasma waves excited by HF pump waves at the plasma and upper hybrid resonance levels. This leads to an electron flux transport along the magnetic field lines. Ohmic heating increases the electron temperature  $T_e$  and the plasma pressure in the modified ionosphere. An increase of the  $T_e$  at heights above the HF pump reflection level can be distinguished in the EISCAT UHF radar data (see Figures 8 and 13). HF pumping may also lead to other possible ac-

celerator mechanisms which occur in the naturally disturbed auroral ionosphere: lower hybrid wave Landau resonance, kinetic Alfvén waves, and anomalous resistivity [Borovsky, 1993; Vogt and Haerendel, 1998].

Let us consider a probable chain of events during the growth phase of a substorm after a stable auroral arc has arrived, and the heater was turned on. Usually, a significant part of the upward current in the arc current system  $j_{z0}^\uparrow$  was carried by precipitating energetic electrons that ionize the ionosphere. In the positive feedback instability scenario, perturbation of the plasma density and that of the upward FAC intensity are tied as  $d\delta N_e/dt \simeq Q\delta j_z^\uparrow$  [ $\text{cm}^{-3}\text{s}^{-1}$ ]. Here  $Q$  is the ionization function of the precipitating flux and  $j_z^\uparrow$  is in  $\text{mA/m}^2$ .

In turn, the perturbation of  $j_z^\uparrow$  carried by an Alfvén wave, is generated over a conductivity perturbation  $\delta\Sigma(\mathbf{r})$ , can be approximated as (e.g., [Kozlovsky and Lyatsky, 1997])

$$\delta j_z \simeq \frac{\Sigma_A}{\Sigma_P} \frac{\delta\Sigma}{\Sigma_{P0}} j_{z0}^\uparrow \simeq \beta j_{z0}^\uparrow \frac{\delta N_e}{N_e} \quad (1)$$

where  $\Sigma_A = 1/\mu_0 V_A$  is the wave conductivity,  $\mu_0$  is the vacuum permeability,  $V_A$  is Alfvén velocity,  $\Sigma_P$  is the height-integrated Pedersen conductivity, and  $\beta \sim 0.1$ . An initial inhomogeneity grows with a characteristic rate (instability increment) of  $\gamma \simeq Q\beta j_{z0}^\uparrow/N_0 \simeq 10^{-3} \text{ s}^{-1}$  for  $Q = (3-10)10^2$ ,  $N_0 = 10^5 \text{ cm}^{-3}$ ,  $j_{z0}^\uparrow = 3-1$ . This implies that waves propagate toward the source of energetic particles without losses and their transit time is short,  $\ll \gamma^{-1}$ . Since  $\gamma^{-1}$  is small compared to the duration of the growth phase, the instability has enough time to develop. Therefore, we point out that the field-aligned current-driven instability will start earlier in the region over the heater-enhanced conductivity patch in the E region of the auroral ionosphere in course of the growth phase when the FAC system is being enhanced. A positive feedback in the magnetosphere-ionosphere coupling was included in order for the initial enhancement to grow further on until the critical value of FAC being achieved.

Another scenario is the excitation of the turbulent Alfvén boundary layer (TABL) in the ionospheric Alfvén resonator (IAR) developed by Trakhtengerts and Feldstein [1991].

The IAR instability increment  $\gamma$  at an arbitrary ionization value of the ionospheric E layer is expressed by ([Trakhtengerts and Feldstein, 1991])

$$\gamma = -\frac{V_{A0}}{L} \frac{\frac{\Sigma_P}{3\Sigma_A}}{1 + \left[\frac{\Sigma_P}{3\Sigma_A}\right]^2} \left(1 - \frac{V_{\text{th}}}{V_0}\right) \quad (2)$$

where  $V_{A0}$  is the Alfvén velocity at the height of maximum plasma concentration,  $L$  is the height of the upper wall of the IAR,  $\Sigma_P$  is the height integrated Pedersen conductivity of the ionosphere,  $\Sigma_A$  is the wave conductivity of the magnetosphere,  $V_0$  is the convection velocity, and  $V_{\text{th}}$  is the minimum threshold velocity of the convection which is necessary for an instability to develop. The main TABL parameters estimated by Trakhtengerts and Feldstein [1991] are the

following: threshold velocity of magnetospheric convection  $V_{\text{th}} \sim 10^4 \text{ cm} \cdot \text{s}^{-1}$ ; the basic turbulence scale of the Alfvén waves is  $\lambda_{\perp} \sim 1.5 \text{ km}$ ; the density of the energy flux concentrated in the Alfvén waves and in the energetic electrons is  $F = 100 \text{ erg} \cdot \text{cm}^{-2} \text{ s}^{-1}$ .

It is believed that Alfvén wave generation during HF pump experiments provides a possibility for the instability excitation in the ionospheric Alfvén resonator (IAR) which is bounded from below by the pump-modified ionospheric  $E$  region, and from above by the region of sharp increase of Alfvén velocities at heights up to one Earth radius. The TABL consists of small-scale Alfvén vortices ( $l \sim 1\text{--}3 \text{ km}$ ) trapped inside IARs. The accumulation of energy in the magnetospheric tail is accompanied by an increase in the laminar magnetospheric convection which, under specific geophysical conditions, can turn into a turbulent state. This mechanism would come into play through the local “switch-on” of the TABL in the selected magnetic flux tube footprinted at Tromsø, due to the dependence of the TABL excitation conditions on the ionospheric  $E$  layer.

The local “switch on” of the turbulent boundary layer may promote the formation of a local magnetospheric current system. This would consist of two field-aligned sheet currents on the northward and southward sides of the heater-modified auroral  $E$  region closed via Pedersen currents in the ionosphere. The configuration of this current system is similar to the second configuration (Type II) of *Boström’s* model [Boström, 1964] with driving forces inside this system. In addition, it drives a Hall current. The formation of a local magnetospheric current system is confirmed by the behavior and features of the auroral arc near Tromsø. From optical data obtained during heater-on periods, the appearance of the local spiral-like or bulge structures in the auroral arcs, typical for the region of the field-aligned currents, can be clearly identified in the vicinity of Tromsø (Plates 2 and 9).

## Summary

Experimental results from multi-instrument observations during Tromsø HF pumping experiments in the night-side auroral  $E$  region indicate that the localization and timing of the auroral activations were related to the injection of powerful HF radio waves transmitted from the Tromsø heating facility. The modification of the ionosphere-magnetosphere coupling leading to the local intensification of the auroral activity may be attributed to the following facts:

1. The transmitted  $O$ -mode “heater” waves reflected from the auroral  $E$  region may give rise to an increase of the ionospheric conductivity in the HF pump-modified  $E$  region. The field-aligned current driven instability will start earlier in the region over the heater-enhanced conductivity patch during the growth phase of the auroral substorm when the FAC’s system is being enhanced. A positive feedback in the magnetosphere-ionosphere coupling was included in order for the initial enhancement to grow further on until the critical

value of the FAC being achieved.

2. Excitation of a turbulent Alfvén boundary layer (TABL) can take place under specific geophysical conditions. The TABL consists of small-scale ( $l \sim 1\text{--}3 \text{ km}$ ) Alfvén vortices trapped inside an ionospheric Alfvén resonator which is bounded from the bottom by the HF pump modified  $E$  region and from the top by the region of sharp increase in the Alfvén velocity at altitudes up to one Earth radius. The local “switch on” of the TABL in the selected magnetic tube can turn the laminar magnetospheric convection into a turbulent state.
3. The local “switch on” of the TABL may promote the formation of a local magnetospheric current system. It consists of two field-aligned sheet currents on the northward and southward sides of the heater-modified auroral  $E$  region, closed via Pedersen currents in the ionosphere.
4. The triggering of local auroral activations by HF pump waves requires specific geophysical conditions, *viz.*, the presence of the accumulation of energy in the magnetospheric tail. The accumulation of energy is accompanied by an increase of the laminar convection which manifests itself in the growth of the electric field, formation of the auroral electrojet, *etc.* In this manner the energy source for the auroral activations remains the interaction between the solar wind and the magnetosphere.

We conclude that the experimental results presented here prove the active rôle of the ionosphere in a substorm process and provide intriguing evidence that the injection of a powerful HF radio beam into an auroral sporadic  $E$  layer may cause the triggering of local auroral activations. Therefore, further experiments of the same character are called for.

**Acknowledgments.** We would like to thank the Director and Staff of the EISCAT Scientific Association for providing the radar data. EISCAT is an International Association supported by Finland (SA), France (CNRS), the Federal Republic of Germany (MPG), Japan (NIPR), Norway (NFR), Sweden (NFR), and the United Kingdom (PPARC). The work of the first three Russian authors (N. B., V. K., and T. B.) was supported by grants from the Swedish Institute (SI) within the Visby Programme. They are also grateful to the Russian Foundation of Fundamental Research, grant 97-05-65443. The Swedish author gratefully acknowledges financial support from the Swedish Natural Sciences Research Council (NFR). The first two (N.B. and V.K.) and sixth author (M.R.) were partly supported by NATO linkage grant, CLG 975069. The IMAGE magnetometer data used in this paper were collected as a German-Finnish-Norwegian-Polish-Russian-Swedish project conducted by the Finnish Meteorological Institute. The first three Russian authors wish to thank the Swedish Institute of Space Physics (Uppsala Division) for the assistance and hospitality they enjoyed during their visit there.

The authors thank Rolf Boström, Thomas Leyser, and Tobia Carozzi for useful discussions and helpful comments.

## References

- Akasofu, S.-I., The development of the auroral substorm, *Planet. Space Sci.*, *12*, 273, 1964.
- Bernhardt, P. A., L. M. Duncan, and C. A. Tepley, Artificial airglow excited by high-power radio waves, *Science*, *242*, 1022–1027, 1988.
- Blagoveshchenskaya, N. F., V. A. Kornienko, A. V. Petlenko, A. Brekke, and M. T. Rietveld, Geophysical phenomena during an ionospheric modification experiment at Tromsø, *Ann. Geophys.*, *16*, 1212–1225, 1998.
- Blagoveshchenskaya, N. F., V. A. Kornienko, A. Brekke, M. T. Rietveld, M. J. Kosch, T. D. Borisova, and M. V. Krylov, Phenomena observed by HF long-distance tools in the HF modified auroral ionosphere during magnetospheric substorm, *Radio Sci.*, *34*, 715–724, 1999.
- Borisov, N., A. Gurevich, K. Papadopoulos, and C. L. Chang, Controlled generation of coherent low frequency ULF/ELF/VLF, *Radio Sci.*, *31*, 859–867, 1996.
- Borovsky, J. E., Auroral arc thicknesses as predicated by various theories, *J. Geophys. Res.*, *98*, 6101–6111, 1993.
- Bösinger, T., K. Kaila, R. Rasinkangas, P. Pollari, J. Kangas, V. Trakhtengerts, and A. Demekhov, An EISCAT study of a pulsating auroral arc: simultaneous ionospheric electron density, auroral luminosity and magnetic field pulsations, *J. Atmos. Terr. Phys.*, *58*, 23–35, 1996.
- Boström, R., A model of the auroral electrojets, *J. Geophys. Res.*, *69*, 4983–4999, 1964.
- Djuth, F. T., R. J. Jost, S. T. Noble, W. E. Gordon, P. Stubbe, H. Kopka, E. Nielsen, R. Boström, H. Derblom, Å. Hedberg, and B. Thidé, Observations of e region irregularities generated at auroral latitudes by a high power radio wave, *J. Geophys. Res.*, *90*, 12,293–12,306, 1985.
- Fejer, J. A., Ionospheric modification and parametric instabilities, *Rev. Geophys. Space Phys.*, *17*, 135–153, 1979.
- Foster, J. C., Substorm onset associated with active experiments, in *Abstracts of the International Conference on Substorms*, p. 173, Lake Hamana, Japan, 1998.
- Getmantsev, G. G., N. A. Zujkov, D. S. Kotik, L. P. Mironenko, N. A. Mityakov, and V. O. Rapoport, Combination frequencies in the interaction between high-power short-wave radiation and ionospheric plasma, *JETP Lett.*, *20*, 101–102, 1974.
- Gurnett, D. A., R. L. Huff, J. D. Menietti, J. L. Burch, and J. D. Winningham, Correlated low-frequency electric and magnetic noise along the auroral field lines, *J. Geophys. Res.*, *89*, 8971–8985, 1984.
- Haerendel, G., Field-aligned currents in the Earth's magnetosphere, in *Physics of magnetic flux ropes*, edited by C. T. Russell, E. R. Priest, and L. C. Lee, Geophysical Monograph 58, pp. 539–553, American Geophysical Union, 1990.
- Henderson, M. G., G. D. Reeves, R. D. Belian, and J. S. Murphree, Observations of magnetospheric substorms occurring with no apparent solar wind / imf trigger, *J. Geophys. Res.*, *101*, 10,773–10,791, 1996.
- Holmgren, G., R. Boström, M. C. Kelley, P. M. Kintner, R. Lundin, U. V. Fahlson, E. A. Bering, and W. R. Sheldon, Trigger, an active release experiment that stimulated auroral particle precipitation and wave emissions, *J. Geophys. Res.*, *85*, 5043–5053, 1980.
- Kamide, Y., and W. Baumjohann, *Magnetosphere-Ionosphere Coupling*, Springer-Verlag, Berlin, Heidelberg, 1993.
- Kan, J., On the cause of substorm expansion onset and the processes driving the substorm expansion phase, *J. Atmos. Terr. Phys.*, *55*, 979–983, 1993.
- Kan, J. R., and W. Sun, Simulation of the westward traveling surge and Pi2 pulsation during substorms, *J. Geophys. Res.*, *90*, 10,911–10,922, 1985.
- Kosch, M. J., T. Hagfors, and E. Nielsen, A new digital all-sky imager experiment for optical auroral studies in conjunction with Scandinavian twin auroral radar experiment, *Rev. Sci. Instr.*, *69*, 578–584, 1998.
- Kozlovsky, A. E., and W. B. Lyatsky, Alfvén wave generation by disturbance of ionospheric conductivity in the field-aligned current region, *J. Geophys. Res.*, *102*, 17,297–17,303, 1997.
- LaBelle, J., M. L. Trimpi, R. Brittain, and A. T. Weatherwax, Fine structure of auroral roar emissions, *J. Geophys. Res.*, *100*, 21,953–21,959, 1995.
- Leyser, T. B., B. Thidé, M. Waldenvik, E. Veszelei, V. L. Frolov, S. M. Grach, and G. P. Komrakov, Downshifted maximum features in stimulated electromagnetic emission, *J. Geophys. Res.*, *99*, 19,555–19,568, 1994.
- Lühr, H., A. Aylward, S. C. Buchert, A. P. abd T. Holmboe, and S. M. Zalewski, Westward moving dynamic substorm features observed with the image magnetometer network and other ground-based instruments, *Ann. Geophys.*, *16*, 425–440, 1996.
- Lui, A. T., and J. S. Murphree, A substorm model with onset location tied to an auroral arc, *Geophys. Res. Lett.*, *25*, 1269–1272, 1998.
- Lyatsky, W., E. G. Belova, and A. B. Pashin, Artificial magnetic pulsations generation by powerful ground-based transmitter, *J. Atmos. Terr. Phys.*, *58*, 407–417, 1996.
- Lyatsky, W. B., and Y. P. Maltsev, *The Magnetosphere-Ionosphere Interaction*, Nauka, Moscow, 1983.
- Lysak, R. L., Electrodynamic coupling of the magnetosphere and ionosphere, *Space Sci. Rev.*, *52*, 33–87, 1990.
- Lysak, R. L., Feedback instability of the ionospheric resonant cavity, *J. Geophys. Res.*, *96*, 1553–1568, 1991.
- McPherron, R. L., C. T. Russell, and M. P. Aubry, Satellite studies of magnetospheric substorms on August 15, 1968: 9. phenomenological model for substorms, *J. Geophys. Res.*, *78*, 3131–3149, 1973.
- Mogilevsky, M., Artificial localization of magnetospheric substorms by a HF heating facility, in *Abstracts of the International Conference 'Dynamics of the magnetosphere and its coupling to the ionosphere on multiple scales from INTERBALL, ISTP satellites and ground-based observations'*, p. 22, Zvenigorod, Russia, 1999.
- Nagatsuma, T., H. Fucunishi, H. Hayakawa, T. Mucai, and A. Matsuoke, Field-aligned currents associated with Alfvén waves in the poleward boundary region of the nightside auroral oval, *J. Geophys. Res.*, *101*, 21,715–21,729, 1996.
- Noble, S. T., F. T. Djuth, R. J. Jost, W. E. Gordon, Å. Hedberg, B. Thidé, H. Derblom, R. Boström, E. Nielsen, P. Stubbe, and H. Kopka, Multiple frequency radar observations of high-latitude E region irregularities in the HF modified ionosphere, *J. Geophys. Res.*, *92*, 13,613–13,627, 1987.
- Rietveld, M., P. Stubbe, and H. Kopka, On the frequency dependence of ELF/VLF waves produced by modulated ionospheric heating, *Radio Sci.*, *24*, 270–278, 1989.
- Rietveld, M., H. Kohl, H. Kopka, and P. Stubbe, Introduction to ionospheric heating at Tromsø—1. Experimental overview, *J. Atmos. Terr. Phys.*, *55*, 577–599, 1993.
- Rostoker, G., The evolving concept of a magnetospheric substorm, *J. Atmos. Terr. Phys.*, *61*, 85–100, 1999.
- Rostoker, G., S.-I. Akasofu, W. Baumjohann, Y. Kamide, and R. L. McPherron, The roles of direct input of energy from the solar wind and unloading of stored magnetotail energy in driving magnetospheric substorms, *Space Sci. Rev.*, *46*, 93–111, 1987.

- Samson, J. C., L. L. Cogger, and Q. Pao, Observations of field line resonances, auroral arcs, and auroral vortex structures, *J. Geophys. Res.*, *101*, 17,373–17,383, 1996.
- Stubbe, P., Review of ionospheric modification experiments in Tromsø, *J. Atmos. Terr. Phys.*, *58*, 349–368, 1996.
- Stubbe, P., H. K. B. Thidé, and H. Derblom, Stimulated electromagnetic emission: A new technique to study the parametric decay instability in the ionosphere, *J. Geophys. Res.*, *89*, 7523–7536, 1984.
- Thidé, B., Stimulated scattering of large amplitude waves in the ionosphere: Experimental results, *Phys. Scripta*, *T30*, 170–180, 1990.
- Thidé, B., H. Kopka, and P. Stubbe, Observations of stimulated scattering of a strong high-frequency radio wave in the ionosphere, *Phys. Rev. Lett.*, *49*, 1561–1563, 1982.
- Thidé, B., H. Derblom, Å. Hedberg, H. Kopka, and P. Stubbe, Observations of stimulated electromagnetic emissions in ionospheric heating experiments, *Radio Sci.*, *18*, 851–859, 1983.
- Thidé, B., Å. Hedberg, J. A. Fejer, and M. P. Sulzer, First observations of stimulated electromagnetic emission at Arecibo, *Geophys. Res. Lett.*, *16*, 369–372, 1989.
- Trakhtengerts, V. Y., and A. Y. Feldstein, Turbulent Alfvén boundary layer in the polar ionosphere, 1. Excitation conditions and energetics, *J. Geophys. Res.*, *96*, 19,363–19,372, 1991.
- Trakhtengerts, V. Y., Private communication, 1999.
- Trefall, H., S. Ullaland, J. Stadsnes, I. Singstad, T. Pytte, K. Brønstad, J. Bjordal, R. H. Karas, R. R. Brown, and J. Münch, Morphology and fine time structure of an early-morning electron precipitation event, *J. Atmos. Terr. Phys.*, *37*, 83–105, 1975.
- Vas'kov, V. V., N. I. Bud'ko, A. V. Kapustina, N. A. Ryabova, G. L. Gdalevich, G. P. Komrakov, and A. N. Maresov, Detection on the Intercosmos-24 satellite of VLF and ELF waves stimulated in the topside ionosphere by the heating facility 'Sura', *J. Atmos. Terr. Phys.*, *60*, 1261–1274, 1998.
- Vogt, J., and G. Haerendel, Reflection and transmission of alfvén waves at the auroral acceleration region, *Geophys. Res. Lett.*, *25*, 277–280, 1998.
- Weatherwax, A. T., J. LaBelle, M. L. Trimpf, and R. A. Treumann, Statistical and case studies of radio emissions observed near  $2f_{ce}$  and  $3f_{ce}$  in the auroral zone, *J. Geophys. Res.*, *100*, 7745–7757, 1995.
- Zhulin, I. A., V. M. Mishin, E. V. Mishin, and V. M. Chmyrev, Possibility of artificial localization of a magnetospheric substorm, *Geomagn. and Aeronomy, Engl. Transl.*, *18*, 377–378, 1978.
- N. F. Blagoveshchenskaya, V. A. Kornienko, T. D. Borisova, R. Yu. Luk'yanova, and O. A. Troshichev, Arctic and Antarctic Research Institute, 38 Bering Street, St. Petersburg 199 397, Russia. (nataly@aari.nw.ru, vikkorn@aari.nw.ru, olegtro@aari.nw.ru)
- B. Thidé, Swedish Institute of Space Physics, Uppsala Division, SE-755 91 Uppsala, Sweden. (bt@irfu.se)
- M. J. Kosch and M. T. Rietveld, Max-Planck-Institut für Aeronomie, D-3411 Katlenburg-Lindau, Germany. (kosch@linax1.mpae.gwdg.de, rietveld@mirage.mpae.gwdg.de)
- E. V. Mishin, MIT Haystack Observatory, Westford, MA01886, USA. (evm@haystack.mit.edu)